In situ measurements of the critical thickness for strain relaxation in AlGaN/GaN heterostructures

S. R. Lee,[a] D. D. Koleske, K. C. Cross, J. A. Floro, and K. E. Waldrip
Sandia National Laboratories, Albuquerque, New Mexico 87185-0601

A. T. Wise and S. Mahajan
Department of Chemical and Materials Engineering, Arizona State University, Tempe, Arizona 85287-6006

(Received 1 July 2004; accepted 25 October 2004)

Using *in situ* wafer-curvature measurements of thin-film stress, we determine the critical thickness for strain relaxation in $Al_xGa_{1-x}N/GaN$ heterostructures with $0.14 \leqslant x \leqslant 1$. The surface morphology of selected films is examined by atomic force microscopy. Comparison of these measurements with critical-thickness models for brittle fracture and dislocation glide suggests that the onset of strain relaxation occurs by surface fracture for all compositions. Misfit-dislocations follow initial fracture, with slip-system selection occurring under the influence of composition-dependent changes in surface morphology. © *2004 American Institute of Physics*. [DOI: 10.1063/1.1840111]

Pseudomorphic $Al_xGa_{1-x}N$ alloys grown on (0001) GaN have tensile in-plane misfit strains ranging from 0 to 2.44%. The elastic energy generated by these misfit strains drives fracture, plastic deformation, and surface instabilities during epitaxial growth of these materials—resulting defects degrade the performance of optoelectronic devices made of these alloys. Consequently, the critical thickness where fracture and dislocation glide become possible in AlGaN/GaN places important limits on the design of device heterostructures. While previous work has measured the critical thickness of $Al_xGa_{1-x}N/GaN$ alloys for $0.10 \leqslant x \leqslant 0.42$,[1,2] and for $x=1$,[3–6] little data exists in between.

In this letter, we report measurements of the critical thickness for strain relaxation in $Al_xGa_{1-x}N/GaN$ epitaxial thin films for $0.14 \leqslant x \leqslant 1$. We compare these experiments to various critical-thickness theories, as well as previous work. The goal is to assess the specific mechanisms that operate at the onset of strain relaxation in AlGaN.

Experiments were carried out using $Al_xGa_{1-x}N/GaN$ heterostructures that were grown on (0001) sapphire by metal-organic chemical-vapor deposition (MOCVD). Growths were performed in a rotating-disk reactor at 1050 °C and 70–140 Torr using trimethylgallium (16–95 μmol/min), trimethylaluminum (28–110 μmol/min), and NH_3 (0.25–9 slpm) precursors in H_2 carrier gas.[7] All AlGaN layers were Si doped ($\sim 2\times10^{18}$ cm^{-3}). Growth rates (1.7 μm/h for GaN; 0.11–0.65 μm/h for $Al_xGa_{1-x}N$) were measured *in situ* using optical reflectance.[8] Thin-film stresses were measured in real time using *in situ* laser-deflectometry measurements of wafer curvature.[9] Following growth, the surface morphology of selected samples was examined using tapping-mode atomic-force microscopy (AFM). The composition and strain of $Al_xGa_{1-x}N$ calibration layers grown at the conclusion of each critical-thickness experiment were measured by x-ray diffraction (XRD) using radial scans of reciprocal space about (0004), $(10\bar{1}1)$, and $(20\bar{2}5)$.

As shown in Fig. 1, special multilayer heterostructures were used to detect the critical thickness for the onset of strain relief. A series of bilayers comprised of $Al_xGa_{1-x}N/GaN$ are grown on top of a GaN pseudosubstrate. In the first bilayer, the AlGaN is chosen to be thinner than the expected critical thickness. In each subsequent bilayer, composition is held fixed while the thickness of the AlGaN is incremented by a constant multiplicative factor (1.3× to 2×, depending on the sample). The GaN probe-layer that completes each bilayer initially grows pseudomorphically on the underlying alloy; thus, an increase in the stress of the GaN signals the onset of strain relaxation in the AlGaN. Each experiment concludes with growth of an AlGaN cap, which is used to calibrate the growth rate and composition.

A subtle point important to later discussion is that the GaN probe-layers can only detect AlGaN strain relaxation that arises from the introduction of misfit dislocations. If the GaN grows pseudomorphically on misfit-free AlGaN, elastic relaxation caused by fracture or roughening of the AlGaN is not seen because coherent overgrowth fills in any cracks or troughs in the AlGaN, which reimposes lateral constraints on the film that return it to the full coherency stress. Direct measurements of the AlGaN stress are precluded by the extremely thin layers of interest, signal-to-noise limitations of the laser deflectometer, and oscillatory artifacts produced by film-thickness gradients.[10]

Figure 2 shows the real-time wafer-curvature data that results for a typical critical-thickness experiment. Note that

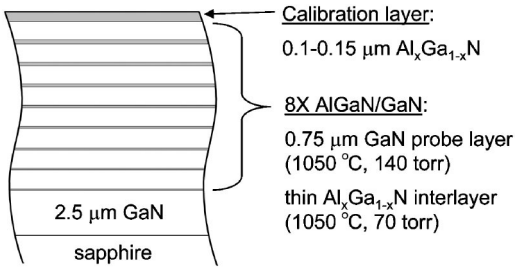

FIG. 1. Schematic diagram of the multilayer samples used to probe the critical thickness for strain relaxation in AlGaN.

[a]Electronic-mail: srlee@sandia.gov

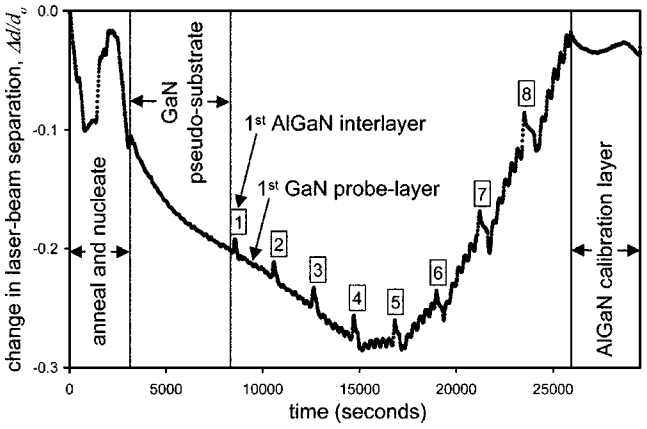

FIG. 2. Stress evolution during the growth of eight $Al_{0.89}Ga_{0.11}N/GaN$ bilayers on GaN. The AlGaN layers sequentially increase in thickness as follows: 1.8, 2.3, 3.0, 3.8, 5.0, 6.5, 8.4, and 11 nm. Each GaN probe-layer is 0.75-μm-thick. Periodic oscillations in the data arise from optical diffraction effects produced by minor film-thickness gradients and are not due to film stress (Ref. 10). Spikes in the data as each AlGaN layer is grown result from reactor pressure changes and are also not due to film stress.

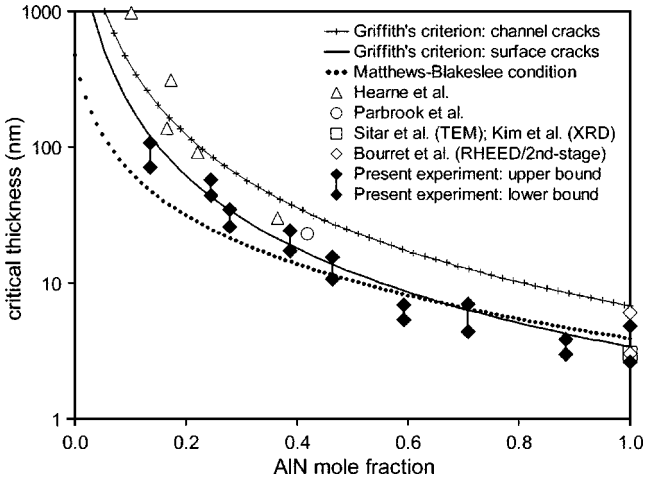

FIG. 3. Comparison of measured critical thicknesses for strain relaxation in $Al_xGa_{1-x}N/GaN$ to both previous measurements and theoretical calculations. For $x<1$, our measurements are for samples grown using an ammonia flow of 1 slpm. For $x=1$, we average results for six samples grown with ammonia flows of 0.25–9 slpm (no trend with ammonia flow was observed).

the normalized change in laser-beam separation ($\Delta d/d_0$) measured in the experiment is proportional to both the wafer curvature ($1/R$) and the stress-thickness product of the thin film (σh_f).[9] Since growth time is proportional to film thickness (h_f), the slope in Fig. 2 measures the film stress. As plotted, negative slopes correspond to tensile stresses. In the figure, the stress is nearly constant from the end of the GaN pseudosubstrate growth to the end of the third GaN probe-layer. Since the GaN stress does not change in this interval, the first three AlGaN interlayers are unrelaxed and pseudomorphic with the surrounding GaN. The fourth probe-layer clearly changes slope, which unambiguously signals the onset of strain relief. Thus, in our example the critical thickness (h_c) is bracketed by the thicknesses of the third and fourth AlGaN interlayers ($3.0\ \text{nm} < h_c \leqslant 3.8\ \text{nm}$). Subsequent AlGaN layers dislocate further with increasing thickness, which drives each GaN probe-layer further into compression, as signified by their rising slopes.

Figure 3 compares a series of these critical-thickness measurements to previously published reports for $Al_xGa_{1-x}N/GaN$ heterostructures; reasonable agreement with prior work is found. For $x<0.42$, our data fall just below results obtained by Hearne *et al.* and Parbrook *et al.*;[1,2] however, we do not observe metastability against fracture for $x<0.18$, as seen by Hearne *et al.* At $x=1.0$, our data bracket results obtained by transmission-electron microscopy (TEM) and XRD,[3,11] but exceed the very small values (0–0.75 nm) obtained by reflection high-energy electron diffraction (RHEED).[4–6] Early RHEED works attribute initial relaxation to rapid dislocation glide,[4,5] but this can be ruled out because glide is prohibited at these low thicknesses by energy-balance considerations. Later RHEED work invokes elastic relaxation produced by a plateletlike surface morphology,[6] which is credible because no critical-thickness limit exists for roughening. Since the GaN probe-layers used in the present work are not sensitive to relaxation caused by surface morphology, this also explains why we do not see a similar "critical thickness." Interestingly, these RHEED studies also report a secondary critical-thickness stage at 3–6 nm.[5,6] This secondary stage agrees with our wafer-curvature observations, and TEM and XRD as well.[3,11]

In an effort to better understand the sequence of mechanisms that operate at the onset of strain relaxation, we calculated theoretical critical-thickness values for three different relaxation processes: (1) brittle fracture by propagation of surface cracks, (2) brittle fracture by propagation of channeling cracks, and (3) plastic deformation by dislocation glide. For brittle fracture, we used Griffith's criterion as formulated by Hutchinson and Suo.[12] For dislocation glide, we used the Matthews–Blakeslee (M–B) condition as formulated by Freund.[13] Additional details specific to AlGaN alloys appear in Ref. 14. Note that our calculations include a nominal correction for the intrinsic growth stress of GaN ($\sim$0.25 GPa),[9] which renders the critical thicknesses finite at $x=0$.

Figure 3 compares these calculations to the experimental data. Turning first to fracture, we note the distinction between surface cracks and channeling cracks.[12] Surface cracks are self-limiting in lateral extent, and thus, may have isolated crack termini. In contrast, channeling cracks are unstable and propagate laterally until they terminate at another crack or the edge of the film. Figure 3 shows that our measured critical thicknesses closely match theory for surface fracture while falling well below theory for channel fracture. Therefore, we infer that surface-fracture initiates relaxation. Importantly, misfit dislocations must very shortly follow; otherwise, there would be no change in stress in the overlying GaN. An ironic consequence of these results is that AlN interlayers used for fracture control in AlGaN/GaN may themselves function through initial fracture.

Figure 3 also shows the Matthews–Blakeslee condition for dislocation glide on the $\frac{1}{3}\langle\overline{1}\overline{1}23\rangle/\{\overline{1}\overline{1}22\}$ slip system,[14,15] which we examine as an alternative to initiation by fracture. This slip system gives a lower bound for the inclined second-order slip systems that are viable in biaxially strained planar alloys grown on (0001) GaN.[14,15] For $x<0.5$, the M–B condition lies below the measured critical thickness, and dislocation glide is initially metastable, in agreement with previous work.[1,14] For $x>0.65$, the M–B condition moves above Griffith's criterion for surface-fracture making surface fracture the favored process. Even so, for $x>0.5$ the proximity of our data to both theories leaves open the possibility that

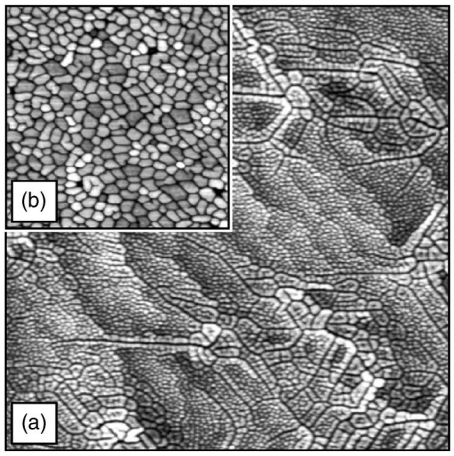

FIG. 4. (a) $2\times2\ \mu m^2$ AFM image of a 9-nm-thick $Al_{0.51}Ga_{0.49}N$ layer grown on GaN using an ammonia flow of 1 slpm. The height scale of the image ranges from 0 nm (black) to 2.5 nm (white). (b) $1\times1\ \mu m^2$ AFM image of a 10-nm-thick AlN layer grown on GaN using an ammonia flow of 6 slpm. The height scale of the image ranges from 0 nm (black) to 4.0 nm (white).

dislocation glide operates first in this regime. On the other hand, we have no evidence that dislocation metastability suddenly ceases for $x>0.5$; moreover, we do have independent evidence for surface fracture in this same regime.

Take, for example, Fig. 4(a), which shows the rich surface morphology found by AFM for a 9-nm-thick layer of $Al_{0.51}Ga_{0.49}N$ on GaN. Several unterminated surface-fracture lines are clearly visible, which verifies that surface fracture does indeed operate at a very early stage. These fractures are of further interest because they are decorated by a complex system of facetted mounds. The mounded regions tend to be thicker than adjacent terraces suggesting an enhanced incorporation rate at locally strain-relaxed regions that bound the fracture lines. Away from fractured areas, surface steps are clearly visible, and a fine-scale dotlike surface morphology covers all of the terraces.

In contrast, Fig. 4(b) shows an AFM image for a 10-nm-thick layer of AlN on GaN. This sample exhibits a more homogeneous surface morphology that is free of steps, fine-scale roughness, and obvious fracture lines; nonetheless, there is tentative evidence for surface fracture here as well. Note that the surface consists of a dense array of facetted or rounded mounds bounded by a network of grooves that are at least $\sim2-4$ nm deep. Many of these mounds are strikingly similar in size and shape to the mounds that decorate the surface fractures in Fig. 4(a), which suggests that surface-fracture may also have lead to the facetted features observed here. Presumably, overt fracture lines have vanished due to the growth and surface transport that follows initial fracture at a critical thickness near 3 nm.

The different surface morphologies seen in Fig. 4(a) versus Fig. 4(b) will influence the slip systems that operate during plastic deformation of the AlGaN. Nonplanar morphologies on the (0001) surface produce inhomogeneous strain fields that enable basal-plane glide of misfit dislocations on the normally inactive $\frac{1}{3}\langle\overline{1}120\rangle/\{0001\}$ primary slip system.[1,14,15] If the bounding grooves are sufficiently deep, the dense array of small mounds seen in Fig. 4(b) would be particulary compatible with this mechanism. In contrast, extended planar surfaces adjacent to crack channels or mounded regions [e.g., the terraces seen in Fig. 4(a)] will have little inhomogeneous strain. In this case, primary slip of misfits is disabled, and only the inclined secondary slip systems can act to propagate interfacial dislocations to regions remote from morphological features such as crack channels or mounds.

In conclusion, we have measured the critical thickness for strain relaxation of $Al_xGa_{1-x}N/GaN$ alloys for the composition range $0.14\leqslant x\leqslant1$. The measurements closely follow Griffith's criterion for surface fracture indicating that surface fracture acts first to initiate relaxation. AFM shows unterminated surface-fracture channels in support of this interpretation. AFM also shows a marked change in surface morphology as composition and ammonia flow are varied. These varying surface morphologies have dissimilar inhomogeneous strains, which influences the slip systems available for dislocation glide. Taken as a whole, our results show that strain relaxation in $Al_xGa_{1-x}N$ alloys proceeds through a complex interplay involving fracture, surface morphology, and dislocation glide.

The authors thank Tom Bauer, Tom Kerley, Mike Russell, and Jeff Figiel for technical assistance. The Office of Basic Energy Sciences at the United States Department of Energy provided partial funding for this study. Lockheed Martin operates Sandia for the United States Department of Energy's National Nuclear Security Administration under Contract No. DE-AC04-94AL85000.

[1] S. J. Hearne, J. Han, S. R. Lee, J. A. Floro, D. M. Follstaedt, E. Chason, and I. S. T. Tsong, Appl. Phys. Lett. **76**, 1534 (2000).
[2] P. J. Parbrook, M. A. Whitehead, R. J. Lynch, and R. T. Murray, Mater. Res. Soc. Symp. Proc. **743**, 505 (2003).
[3] Z. Sitar, M. J. Paisley, B. Yan, J. Ruan, W. J. Choyke, and R. F. Davis, J. Vac. Sci. Technol. B **8**, 316 (1990).
[4] N. Grandjean and J. Massies, Appl. Phys. Lett. **71**, 1816 (1997).
[5] G. Feuillet, B. Daudin, F. Widmann, J. L. Rouviere, and M. Arlery, J. Cryst. Growth **189/190**, 142 (1998).
[6] A. Bourret, C. Adelmann, B. Daudin, J. L. Rouviere, G. Feuillet, and G. Mula, Phys. Rev. B **63**, 245307 (2001).
[7] D. D. Koleske, A. J. Fischer, A. A. Allerman, C. C. Mitchell, K. C. Cross, S. R. Kurtz, J. J. Figiel, K. W. Fullmer, and W. G. Breiland, Appl. Phys. Lett. **81**, 1940 (2002).
[8] W. G. Breiland and K. P. Killeen, J. Appl. Phys. **78**, 6726 (1995).
[9] S. Hearne, E. Chason, J. Han, J. A. Floro, J. Figiel, J. Hunter, H. Amano, and I. S. T. Tsong, Appl. Phys. Lett. **74**, 356 (1999).
[10] W. G. Breiland, S. R. Lee, and D. D. Koleske, J. Appl. Phys. **95**, 3453 (2004).
[11] C. Kim, I. K. Robinson, J. Myoung, K. Shim, M.-C. Yoo, and K. Kim, Appl. Phys. Lett. **69**, 2358 (1996).
[12] J. W. Hutchinson and Z. Suo, *Advances in Applied Mechanics* (Academic, San Diego, 1992), Vol. 29, pp. 63–191.
[13] L. B. Freund, J. Mech. Phys. Solids **38**, 657 (1990).
[14] J. A. Floro, D. M. Follstaedt, P. Provencio, S. J. Hearne, and S. R. Lee, J. Appl. Phys. (accepted).
[15] S. Srinivasan, L. Geng, R. Liu, F. A. Ponce, Y. Narukawa, and S. Tanaka, Appl. Phys. Lett. **83**, 5187 (2003).